

В статті запропоновано використувувати оптоволокно на фотонних кристалах з дефектом внутрішньої порожнини. На використання таких волокон не впливає матеріальний засіб на поширенні оптичної радіації. Фотонні кристали володіють спеціальними властивостями та можливостями, які призводять до величезного потенціалу для застосування зондування

Ключові слова: оптичний гіроскоп, оптоволокно на фотонних кристалах, ефект Саньяка

В статье предложено использовать оптоволокно на фотонных кристаллах с дефектом внутренней полости. На использование таких волокон не воздеиствует материальное средство на распространении оптической радиации. Фотонные кристаллы обладают специальными свойствами и возможностями, которые приводят к огромному потенциалу для приложений зондирования

Ключевые слова: оптический гироскоп, оптоволокно на фотонных кристаллах, эффект Саньяка

UDC: 621.373.826
DOI: 10.15587/1729-4061.2015.37799

FIBER-OPTIC GYROSCOPES BASED ON PHOTONIC-CRYSTAL FIBERS

Haider Ali Muse

Postgraduate student

Faculty of electronic engineering

Department of Physical Foundations
of Electronic Engineering

Kharkiv national university of radio electronics
Lenina ave., 14, Kharkov, Ukraine, 61000

Hadr_2005@yahoo.com

1. Introduction

Fiber optic gyroscopes (FOG) are generally recognized as promising for the control and navigation systems moving objects of various kinds (ground transportation, ships, aircraft, etc.). At the same time demand are (fiber optical gyroscope) in a wide range of characteristics of accuracy – 10.0 deg/h to 0, 001 deg/hr. In Russia, the leader in the production of a number of FOG accuracy class 10.0–1.0 deg/h is LLC “Physoptic”. However, there is a gap from the foreign generally recognized as FOG for the control and navigation systems moving objects of various kinds level in FOG navigational accuracy class (0.01–0.001 deg/h). Performance characteristics of fiber-optic gyroscope increased accuracy are largely dependent on the characteristics of its basic elements and features of its assembly techniques. Thus, the development of fiber-optic gyroscope and methods of its production is an urgent task. Due to their unique geometric structure, photonic crystal fibers present special properties and capabilities that lead to an outstanding potential for sensing applications. The diversity of unusual features of photonic crystal fibers, beyond what conventional fibers can offer, leads to an increase of possibilities for new and improved sensors. There is a huge interest of the scientific community in this original technology for applications in a variety of fields. The aim of this work was to conduct theoretical studies of the conditions of photonic crystal fiber (PCF) usage as a part of the fiber optical gyroscope. Photonic crystal fiber gyroscopes are a kind of optics gyroscopes that present a diversity of new and improved features beyond what conventional optical fiber gyroscopes can offer.

2. Analysis of published data and problem statement

With the development of optoelectronic technology [1], optical fibers have been intensively investigated at

various sensor fields owing to their unique characteristics such as multiplexing, remote sensing, high flexibility, low propagating loss, high sensitivity, low fabrication cost, small form factor, high accuracy, simultaneous sensing ability, and immunity to electromagnetic interference. This is the case of Photonic Crystal Fibers (PCFs), also called holey fibers, which contain arrays of tiny air holes along their structure and allow, among other new applications, the fabrication of new optical fiber sensors. Thanks to the flexibility for the cross section design, photonic crystal fibers (PCFs) [2, 3] have achieved excellent properties in birefringence [4, 5], dispersion [6, 7], single polarization single mode [8, 9], nonlinearity [10], and effective mode area [11, 12], and also excellent performances in the applications of fiber sensors [13, 14], fiber lasers [15, 16] and nonlinear optics [17, 18] over the past several years. Large numbers of research papers have highlighted some optical properties of the PCFs such as ultrahigh birefringence and unique chromatic dispersion, which are almost impossible for the conventional optical fibers. A few years later in 1991, Yablonovitch and co-workers produced the first photonic crystal by mechanically drilling holes a millimeter in diameter into a block of material with a refractive index of 3.6 [19]. In 1995, Birks et al. proposed a fiber with air holes along its length that could guide light through this structure with interesting properties [20, 21]. Nowadays the PCF has become a subject of extensive research and has opened a new range of possible applications. The structure of the PCF enables to have different types of fibers such as endless single mode, double clad, germanium or rare earth doped, high birefringence, and many others with particular features due to its manufacturing flexibility. This variety of choices permits the use of PCF in numerous applications such as sensors which measure physical parameters (temperature, pressure, force, etc.), chemical compounds in gas and liquids, and even biosensors [22, 23].

3. Purpose and objectives of the study

The main aim of this paper is using photonic crystal fiber as part of the gyroscopes because there are many reasons as shown below

A wide variety of fiber-optic-based sensing schemes have been proposed and reported to date, such schemes have a number of disadvantages such as high coupling losses, limited mechanical reliability, and difficulties in mass production. Photonic crystal fibers should present properties such as small size, simple design, and an all-fiber configuration with high measurement accuracy.

Photonic crystal fibers are used because unlike their conventional counterparts, Photonic crystal fiber-based sensing techniques minimally disturb the electric or magnetic field, and apart from the sensor head, the connecting fibers are inherently immune to electromagnetic interference. Also, they can provide true dielectric isolation between the sensor and the interrogation system in the presence of very high electromagnetic fields.

According to these features we can elimination a lot of the problems that exist in the conventional fiber optic gyroscope and getting better and more accurate results in the same conditions when using Photonic Crystal Fibers.

4. Sagnac Interferometer fibers

Sagnac interferometers (SIs) are recently in great interest in various sensing applications owing to their advantages of simple structure, easy fabrication, and environmental robustness [24]. SI consists of an optical fiber loop, along which two beams are propagating in counter directions with different polarization states. As schematically illustrated in Fig. 1, the input light is split into two directions by a 3dB fiber coupler and the two counter-propagating beams are combined again at the same coupler. Unlike other fiber optic interferometers, the OPD is determined by the polarization dependent propagating speed of the mode guided along the loop. To maximize the polarization-dependent feature of SIs, birefringent fibers are typically utilized in sensing parts. The polarizations are adjusted by a polarization controller (PC) attached at the beginning of the sensing fiber. The signal at the output port of the fiber coupler is governed by the interference between the beams polarized along the slow axis and the fast axis. The phase of the interference is simply given as:

$$\delta = \frac{2\pi}{\lambda}BL, \tag{1}$$

$$B = |n_f - n_s|.$$

Where B is the birefringent coefficient of the sensing fiber, L is the length of the sensing fiber, and n_f and n_s are the effective indices of the fast and slow modes, respectively [24].

Fig. 1 is schematic of the sensor based on a Sagnac interferometer. In general, high birefringent fibers (HBFs) or polarization maintaining fibers (PMFs) are chosen as the sensing fibers to acquire high phase sensitivity. For the temperature sensing application, the fiber is doped to have a large thermal expansion coefficient, which induces high birefringence variation [25]. When measuring others

parameters such as strain, pressure, and twist, however, the high birefringent characteristics of the HBFs and PMFs can depreciate the sensing ability due to their strong temperature dependency [26, 27]. In order to overcome this problem, polarization-maintaining photonic crystal fibers (PMPCFs) have been introduced as the sensing fibers. The pure silica-based PCF is good to have thermal robustness; but the air-hole structure of the PCF should be adjusted to have high birefringence [28, 29]. Furthermore, since the polarization modes of the fiber are sensitive to the bending of the fiber due to the asymmetric fiber structure, a high-sensitive curvature sensor could be reported based on a simple SI setup [30].

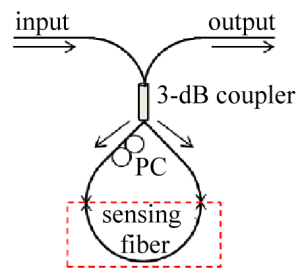


Fig. 1. Sensor based on a Sagnac interferometer

5. Basic conditions of work of fiber optical gyroscope

Fiber optical gyroscope is based on the Sagnac effect [31]. Sagnac effect generates an optical phase difference, $\Delta\phi$, between two counter propagating waves in a rotating fiber coil (optical path)[32]:

$$\Delta\phi = \frac{8\pi S}{\lambda c} \Omega, \tag{2}$$

where $(\Delta\phi)$ – phase difference, Ω – angular velocity, C – light –/signal velocity, λ – wavelength, S – scale factor.

Fig. 2 open-loop (FOG) is the simplest and lowest cost rotation sensors. They are widely used in commercial applications where their dynamic range and linearity limitations are not constraining.

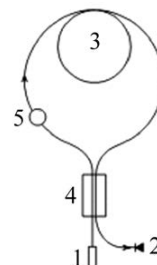


Fig. 2. Scheme of fiber optic gyroscope

However, a clear and precise definition of the angular velocity is necessary to exclude the possibility of additive and multiplicative effects of other physical effects on the measured value of the phase difference of counter propagating waves. The main challenge to the realization of high-precision phase measurements is a zero drift, which is

manifested in the fact that physically stationary gyroscope output signal there, which is due to physical phenomena not related to the rotation of the loop. In the fiber material in a medium to obtain a stable optical phase oscillations is practically impossible. Therefore fiber optic gyroscopes may occur an additive phase noise. One of the reasons for the appearance of these signals is the scattering and reflection in a fiber loop. During the rotation angular velocity contour (Ω), an apparent distance between points A and B for the oppositely traveling beams changes. For a wave traveling from point A to point B, i.e., in direction similar to the direction of rotation of the contour, the distance is extended, as in a time dt point B moves to the angle ($d\varphi = \Omega \cdot dt$), go to point C. This is for lengthening the path of the light beam is equal to $v \cdot dt$, since at each instant the beam is directed at a tangent to the contour at that same tangential linear velocity directed projection ($\vec{v} = \vec{v} \cdot \cos \alpha = \Omega \cdot r \cdot \cos \alpha$). Thus, the length of the path traversed by the beam is equal to $Dl + v \cdot dt$. Arguing similarly, for opposing traveling light beam will be a reduction in the apparent path segment $Dl - v \cdot dt$. Considering the speed of light invariant quantity, apparent elongation and reduction paths for opposing beams can be considered equivalent to extensions and contractions of time intervals, i.e.,

$$\Delta t_1 = \frac{1}{c} (\Delta l + v \cdot dt), \tag{3}$$

$$\Delta t_2 = \frac{1}{c} (\Delta l - v \cdot dt). \tag{4}$$

If the relative time delay of counter propagating waves occurring during the rotation, expressed in terms of the phase difference of counters propagating waves, it will be

$$\Delta \varphi = \omega \cdot \Delta t = \frac{4 \cdot \omega \cdot S}{c^2} \cdot \Omega = \frac{8 \cdot \pi \cdot v \cdot S}{c^2} \cdot \Omega = \frac{8 \cdot \pi \cdot S}{\lambda \cdot c}, \tag{5}$$

where $\omega = 2 \cdot \pi \cdot \nu$

$$\lambda = \frac{c}{\nu}.$$

Basic conditions of work of listed FOG not allow us to understand the constraints that are imposed on the accuracy of measurements made with it. Hitherto used fiber optic gyroscopes quartz fibers used in optical communications. In these fibers, that are amorphous, almost homogeneous and isotropic medium can propagate transverse optical waves. Light reflected from the interface «core-shell» as a result of total internal reflection propagates along the core as its own wave of the optical waveguide. Light wave as electromagnetic wave propagates along the fiber with a phase velocity is inversely proportional to the refractive index. Even a weak inhomogeneity can lead to cumulative effect and change the measurement result. Since the optical radiation propagates in a material medium, and it refers to the optical fiber, which is made of quartz or quartz glass, such physical phenomena as the birefringence effect, Kerr effect, Faraday effect, etc. adversely affect the angle of rotation loop fiber optic gyroscopes and registered phase of the optical signal. These effects associated with the process of optical radiation propagation in the material of the optical medium, leading to a phase shift of counter propagating waves, which is not

associated with the rotation of the closed loop. The negative effects are also associated with the processes of scattering and reflection of light in an optical path, the polarization non-reciprocity effect associated with the asymmetric arrangement of anisotropic elements, relative to the centre of the fiber loop, or anisotropic fiber properties. However, the main problem of the FOG is that as the measuring accuracy and reducing the magnitude of the angular velocity measured is increasingly influenced by the optical effects not related to the angular displacement of the optical loop (FOG). Since the optical radiation propagates in a material medium, and it refers to the optical fiber, which is made of quartz or quartz glass, such physical phenomena as the birefringence effect, Kerr effect, Faraday effect, etc. adversely affect the angle of rotation loop fiber optic gyroscopes and registered phase of the optical signal. These effects associated with the process of optical radiation propagation in the material of the optical medium, leading to a phase shift of counter propagating waves, which is not associated with the rotation of the closed loop. The negative effects are also associated with the processes of scattering and reflection of light in an optical path, the polarization non-reciprocity effect associated with the asymmetric arrangement of anisotropic elements, relative to the centre of the fiber loop, or anisotropic fiber properties. This problem was solved, and solved by the use of frequency and phase modulation of the optical radiation is used, which allows to shift the zero point on the slope with the maximum slope of the interference signal. However, to get rid of the phase shifts, non-rotation circuit fails. Effects associated with locally mutual, non-stationary changes in the parameters of fiber, when they are excited asymmetrically with respect to the middle of the fiber loop. The main effects are the Faraday effect, Fresnel - Fizeau and nonlinear optical Kerr effect. The use of non-monochromatic radiation SLD (super luminescent diode with a coherence length of 10–20 microns) is practically eliminates the problem of the influence of the reflected and scattered radiation on the phase of the output signal of the FRI. However, the use of SLD removed only part of the problems leading to additional signals.

6. Photonic crystal fiber (PCF)

A photonic crystal fiber is an optical fiber which obtains its waveguide properties not from a spatially varying glass composition but from an arrangement of very tiny and closely spaced air holes which go through the whole length of fiber. Such air holes can be obtained by using a preform with (larger) holes, made e. g. by stacking capillary and/or solid tubes (stacked tube technique) and inserting them into a larger tube. Usually, this preform is then first drawn to a cane with a diameter of e. g. 1 mm, and thereafter into a fiber with the final diameter of e. g. 125 μm . Particularly soft glasses and polymers (plastics) also allow the fabrication of preforms for photonic crystal fibers by extrusion [33, 34]. There is a great variety of hole arrangements, leading to PCFs with very different properties. All these PCFs can be considered as specialty fibers. In this paper used the fibers of the type Hollow Core photonic crystal fiber, 1550 nm, $\varnothing 10 \mu\text{m}$, core Hollow core Photonic Bandgap Fibers guide light in a hollow core, surrounded by a microstructured cladding of air holes and silica. Fig. 3 illustrated typical attenuation and dispersion.

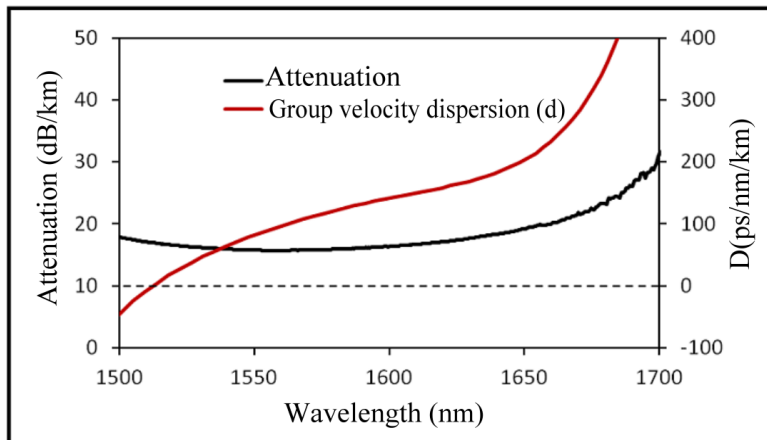


Fig. 3. Typical attenuation and dispersion

Since only a small fraction of the light propagates in silica, the effect of material nonlinearities is insignificant and the fibers do not suffer from the same limitations on loss as conventional fibers made from solid material alone.

7. Principles of operation of ring interferometer based on photonic crystal fibers

The main argument in favor of a replacement optical fiber to another medium, is that the first Sagnac experiments conducted in the hollow pipe and the low pressure air is not observed effects are manifested in the optical fiber. In this regard, it is evident that the use of such optical media, which on the one hand, would allow optical radiation to channel, and on the other hand did not change to its frequency and phase characteristics. Such environments include photonic crystals with defects. In such environments, the defect is a hollow waveguide. Manufactured photonic crystal fiber has a refractive index of 1.82 at wavelength 500 nm for this fiber type Kagome effective single-mode propagation occurs in a wavelength range from 750 to 1050 nm in diameter mainly 30 micro and loss of about 0.7 dB/m [35] see Fig. 4.

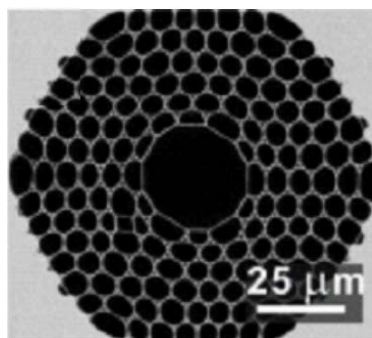


Fig. 4. An example of photonic crystal fiber with a hollow core diameter of about 30 microns

The collapsed zones in the PCF cause a broadening of the beam when it propagates from the SMF to the PCF [36, 37]. The broadening of the beam combined with the axial symmetry and the modal properties of the PCF are what allow the excitation (and recombination) of modes that have similar azimuthal symmetry [38]. The modes

excited in the PCF have different effective indices (or different propagation constants), thus they travel at different speeds. As a result, the modes accumulate a phase difference as they propagate along the PCF. Due to the excitation and recombination of modes in the device, the reflection spectrum is expected to exhibit a series of maxima and minima (interference pattern). When two modes participate in the interference the transmitted or reflected intensity (*I*) can be expressed as:

$$I = I_1 + I_2 + 2\sqrt{I_1 I_2} \cos(\Delta\Phi). \tag{6}$$

In Equation (6) *I*₁ and *I*₂ are, respectively, the intensity of the core mode and the cladding mode and $\Delta\Phi = 2\pi\Delta n L / \lambda$ is the total phase shift.

$\Delta n = n_f - n_c$, n_f and n_c being, respectively, the effective refractive index of the core mode and the cladding mode. *L* is the physical length of the PCF and λ the wavelength of the optical source. The fringe spacing or period (*P*) of the interference pattern is given by $P = \lambda^2 / (\Delta n L)$. The maxima of the interference pattern appear at wavelengths that satisfy the condition $\Delta\Phi = 2m\pi$, with $m = 1, 2, 3, \dots$. This means at wavelengths given by

$$\lambda_m = \Delta n \frac{L}{m}. \tag{7}$$

The fringe contrast or visibility (*V*) of a modal interferometer is an important parameter, particularly when the interferometer is used for sensing applications. Typically, higher visibility is desirable since it leads to larger signal-to-noise ratio and more accurate measurement. The visibility of a two-mode interferometer can be calculated by the well-known expression: $V = (I_{max} - I_{min}) / (I_{max} + I_{min})$, where *I*_{max} and *I*_{min} are, respectively, the maximum and minimum values of *I* given in Equation (6). According to the definition and equation (6) *V* can be expressed as [39]:

$$V = \frac{2\sqrt{k}}{(1+k)}, \tag{8}$$

where $k = I_1 / I_2$.

Many research groups prefer fringe contrast (expressed in dB) instead of visibility. The fringe contrast (*FC*) is defined here as $FC = -10\log(1 - V)$. In Figure 5 we show the dependence of the fringe contrast on *k* along with the theoretical interference pattern of device with *L* = 10 mm for two values of *k*. It can be noted that the fringe contrast increases as *k* approaches 6, i. e., when the two modes that participate in the interference have equal intensities (Fig. 5). Fringe contrast in a mode of interferometer as a function of *k* or the intensity of the cladding mode to that of the core mode ratio. The inset shows the theoretical reflection spectrum in the case of $k = 0.4$ (dotted line) and $k = 0.96$ (solid line).

The physical mechanism for the waveguide propagation of radiation in photonic fibers is not associated with the phenomenon of total internal and with the presence of the photonic band gap in the transmission spectrum of the fiber cladding. Waveguides of this type are promising for the creation of gas sensors, spectral elements, as well

as laser-cooled atoms management. Experimental studies have shown that in some cases [40] relatively high loss optical fibers with core air owing to scattering of light by irregularities of the glass surface due to the capillary waves frozen. Solution to reduce optical loss photonic fibers requires further fundamental research, however, we can already use small pieces of photonic fibers in special measuring instruments, which include the FOG. Photonic crystal fiber is a two-dimensional photonic crystal structure based on the song “quartz glass-to-air” formed in the shell.

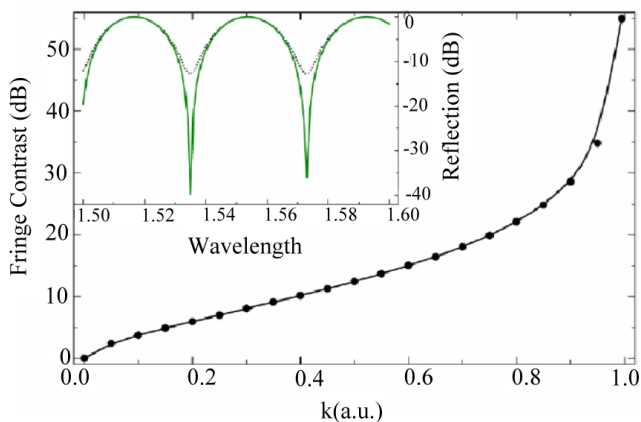


Fig. 5. Fringe contrast in a mode of interferometer

8. Propagation of optical radiation in photonic crystal defect

In [41] were considered in detail the conditions of formation of photonic crystal fibers and spread them in the optical radiation. Experimental studies of PCF were conducted in a number of studies, for example, [42]. Photonic band gaps arising in the transmission spectrum of a two-dimensional periodic cladding, provides a high reflection coefficient for radiation propagating along the hollow core, realizing mode waveguide propagation. In [42] the results of an experimental determination of the optical emission intensity distribution in the cross-sectional center of the defect and the results of numerical calculation of the distribution of power density in cross-section are given. These results are shown in Fig. 6.

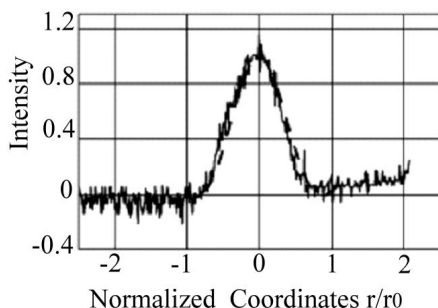


Fig. 6. Distribution of the output power with a hollow core PCF (solid line), numerical calculation of the intensity distribution (dashed line)

Fig. 7 illustrated the typical near field intensity profile.

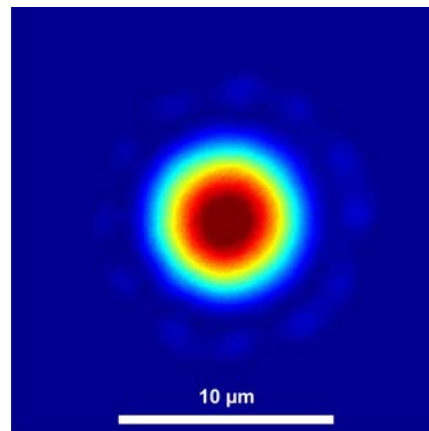


Fig. 7. Typical near field intensity profile

To date, published studies on the conditions of PCF usage for transmitting optical information signals in telecommunication systems, however, the use of PCF in optical interferometers have only begun to explore, for precision measurements of some physical quantities. In [43] the results of measurement of voltage using a cylindrical PCF, which is formed by the interferometer, are given. To describe the operation of a fiber gyroscope based on PCF must use the description of the optical waves propagating along the two-dimensional photonic crystal defect [44]. To implement the necessary PCF fiber gyroscope with a minimum loss of less than 1 dB/km, that extends single-mode radiation. These fibers include, for example, commercially available PCF – HC19-1550 (0,03 dB\km) or LMA –25 (1,5 dB\km) operating at 1550 nm. The low level of absorption in these fibers allows you to create on their basis multiturn ring interferometer, which implements the Sagnac effect. The main technical challenge in applying PCF is the junction of the individual elements of the PCF, Here are some distinctive features of the assembly fiber interferometer.

9. Conclusion

Due to their unique geometric structure, photonic crystal fibers present special properties and capabilities that lead to an outstanding potential for sensing applications.

The report discusses the conditions of realization of the structure of the fiber gyroscope using a photonic crystal fiber. With this fiber, and methods and devices for forming fiber interferometers, can be solved the problem of creating a fiber-optic gyroscope based on photonic – crystal fiber.

References

1. Overview of Fiber Optic Sensors [Electronic resource] / Available at: http://www.bluerr.com/images/Overview_of_FOS2.pdf (Last accessed: 8.02.2012).
2. Knight, J. C. All-silica single-mode optical fiber with photonic crystal cladding [Text] / J. C. Knight, T. A. Birks, P. S. J. Russell, D. M. Atkin // Optics Letters. – 1996. – Vol. 21, Issue 19. – P. 1547–1549. doi: 10.1364/ol.21.001547
3. Chau, Y.-F. A comparative study of high birefringence and low confinement loss photonic crystal fiber employing

- elliptical air holes in fiber cladding with tetragonal lattice [Text] / Y.-F. Chau, C.-Y. Liu, H.-H. Yeh, D. P. Tsai // Progress In Electromagnetics Research B. – 2010. – Vol. 22. – P. 39–52. doi: 10.2528/pierb10042405
4. Ortigosa-Blanch, A. Highly birefringent photonic crystal fibers [Text] / A. Ortigosa-Blanch, J. C. Knight, W. J. Wadsworth, J. Arriaga, B. J. Mangan, T. A. Birks, P. S. J. Russell // Optics Letters. – 2000. – Vol. 25, Issue 18. – P. 1325–1327. doi: 10.1364/ol.25.001325
 5. Chen, D. Ultrahigh birefringent photonic crystal fiber with ultralow confinement loss [Text] / D. Chen, L. Shen // IEEE Photonics Technology Letters. – 2007. – Vol. 19. – P. 185–187. doi: 10.1109/lpt.2006.890040
 6. Agrawal, A. Golden spiral photonic crystal fiber: Polarization and dispersion properties [Text] / A. Agrawal, N. Kejalakshmy, J. Chen, B. M. A. Rahman, K. T. V. Grattan // Optics Letters. – 2008. – Vol. 33, Issue 22. – P. 2716–2718. doi: 10.1364/ol.33.002716
 7. Yang, S. Theoretical study and experimental fabrication of high negative dispersion photonic crystal fiber with large area mode field [Text] / S. Yang, Y. Zhang, X. Peng, Y. Lu, S. Xie, J. Li, W. Chen, Z. Jiang, J. Peng, H. Li // Optics Express. – 2006. – Vol. 14, Issue 7. – P. 3015–3023. doi: 10.1364/oe.14.003015
 8. Ju, J. Design of single-polarization single mode photonic crystal fibers [Text] / J. Ju, W. Jin, M. S. Demokan // J. Lightwave Technol. – 2001. – Vol. 24. – P. 825–830.
 9. Kubota, H. Absolutely single polarization photonic crystal fiber [Text] / H. Kubota, S. Kawanishi, S. Koyanagi, M. Tanaka, S. Yamaguchi // IEEE Photonics Technology Letters. – 2004. – Vol. 16, Issue 1. – P. 182–184. doi: 10.1109/lpt.2003.819415
 10. Knight, J. C. Nonlinear waveguide optics and photonic crystal fibers [Text] / J. C. Knight, D. V. Skryabin // Optics Express. – 2007. – Vol. 15. – P. 15365–15376. doi: 10.1364/oe.15.015365
 11. Mortensen, N. A. Improved large-mode-area endlessly single mode photonic crystal fibers [Text] / N. A. Mortensen, M. D. Nielsen, J. R. Folkenberg, A. Petersson, and H. R. Simonsen // Optics Letters. – 2003. – Vol. 28, Issue 6. – P. 393–395. doi: 10.1364/ol.28.000393
 12. Folkenberg, J. Polarization maintaining large mode area photonic crystal fiber [Text] / J. Folkenberg, M. Nielsen, N. Mortensen, C. Jakobsen, and H. Simonsen // Optics Express. – 2004. – Vol. 12, Issue 5. – P. 956–960. doi: 10.1364/opex.12.000956
 13. Dobb, H. Temperature-insensitive long period grating sensors in photonic crystal fibre [Text] / H. Dobb, K. Kalli, D. J. Webb // Electronics Letters. – 2004. – Vol. 40, Issue 11. – P. 657–658. doi: 10.1049/el:20040433
 14. Dong, X. Temperature-insensitive strain sensor with polarization-maintaining photonic crystal fiber based on Sagnac interferometer [Text] / X. Dong, H. Y. Tam // Applied Physics Letters. – 2007. – Vol. 90, Issue 15. – P. 151113. doi: 10.1063/1.2722058
 15. Wadsworth, W. J. Yb³⁺-doped photonic crystal fibre laser [Text] / W. J. Wadsworth, J. C. Knight, W. H. Reewes, P. S. J. Russell, J. Arriaga // Electronics Letters. – 2000. – Vol. 36, Issue 17. – P. 1452–1453. doi: 10.1049/el:20000942
 16. Chen, D. Stable multi-wavelength erbium-doped fiber laser based on photonic crystal fiber Sagnac loop filter [Text] / D. Chen // Laser Physics Letters. – 2007. – Vol. 4, Issue 6. – P. 437–439. doi: 10.1002/lapl.200710003
 17. Broderick, N. G. R. Nonlinearity in holey optical fibers: Measurement and future opportunities [Text] / N. G. R. Broderick, T. M. Monro, P. J. Bennett, D. J. Richardson // Optics Letters. – 1999. – Vol. 24, Issue 20. – P. 1395–1397. doi: 10.1364/ol.24.001395
 18. Dudley, J. M. Ten years of nonlinear optics in photonic crystal fibre [Text] / J. M. Dudley, J. R. Taylor // Nature Photonics. – 2009. – Vol. 3, Issue 2. – P. 85–90. doi: 10.1038/nphoton.2008.285
 19. Yablonovitch, E. Photonic Band Structure: The Face-Centered-Cubic Case Employing Nonspherical Atoms [Text] / E. Yablonovitch, T. J. Gmitter, K. M. Leung // Physical Review Letters. – 1991. – Vol. 67, Issue 17. – P. 2295–2298. doi: 10.1103/physrevlett.67.2295
 20. Birks, T. A. Full 2-D photonic bandgaps in silica/air structures [Text] / T. A. Birks, P. J. Roberts, P. S. J. Russell, D. M. Atkin, and T. J. Shepherd // Electronics Letters. – 1995. – Vol. 31, Issue 22. – P. 1941–1943. doi: 10.1049/el:19951306
 21. Knight, J. C. All-silica single-mode optical fiber with photonic crystal cladding [Text] / J. C. Knight, T. A. Birks, P. S. J. Russell, D. M. Atkin // Optics Letters. – 1996. – Vol. 21, Issue 19. – P. 1547–1549. doi: 10.1364/ol.21.001547
 22. Ho, H. L. Optimizing microstructured optical fibers for evanescent wave gas sensing [Text] / H. L. Ho, Y. L. Hoo, W. Jin, J. Ju, D. N. Wang, R. S. Windeler, Q. Li // Sensors and Actuators B. – 2007. – Vol. 122, Issue 1. – P. 289–294. doi: 10.1016/j.snb.2006.05.036
 23. Bock, W. J. A photonic crystal fiber sensor for pressure measurements [Text] / W. J. Bock, J. Chen, T. Eftimov, W. Urbanczyk // IEEE Transactions on Instrumentation and Measurement. – 2006. – Vol. 55, Issue 4. – P. 1119–1123. doi: 10.1109/tim.2006.876591
 24. Fu, H. Y. Pressure sensor realized with polarization-maintaining photonic crystal fiber-based Sagnac interferometer [Text] / H. Y. Fu, H. Y. Tam, L. Y. Shao, X. Dong, P. K. A. Wai, C. Lu, S. K. Khijwania // Applied Optics. – 2008. – Vol. 47. – P. 2835–2839. doi: 10.1364/ao.47.002835
 25. Moon, D. S. The temperature sensitivity of Sagnac loop interferometer based on polarization maintaining side-hole fiber [Text] / D. S. Moon, B. H. Kim, A. Lin, G. Sun, T. G. Han, W. T. Han, Y. Chung // Optics Express. – 2007. – Vol. 15, Issue 13. – P. 7962–7967. doi: 10.1364/oe.15.007962

26. Kim, G. Strain and temperature sensitivities of an elliptical hollow-core photonic bandgap fiber based on Sagnac interferometer [Text] / G. Kim, T. Cho, K. Hwang, K. Lee, K. S. Lee, Y. G. Han, S. B. Lee // *Optics Express*. – 2009. – Vol. 17, Issue 4. – P. 2481–2486. doi: 10.1364/oe.17.002481
27. Kim, H. M. Enhanced transverse load sensitivity by using a highly birefringent photonic crystal fiber with larger air holes on one axis [Text] / H. M. Kim, T. H. Kim, B. Kim, Y. Chung // *Applied Optics*. – 2010. – Vol. 49, Issue 20. – P. 3841–3845. doi: 10.1364/ao.49.003841
28. Dong, B. Cladding-mode resonance in polarization-maintaining photonic-crystal-fiber-based sagnac interferometer and its application for fiber sensor [Text] / B. Dong, J. Hao, C. Y. Liaw, Z. Xu // *Journal of Lightwave Technology*. – 2011. – Vol. 29, Issue 12. – P. 1759–1763. doi: 10.1109/jlt.2011.2140313
29. Kim, D. H. Sagnac loop interferometer based on polarization maintaining photonic crystal fiber with reduced temperature sensitivity [Text] / D. H. Kim, J. U. Kang // *Optics Express*. – 2004. – Vol. 12, Issue 19. – P. 4490–4495. doi: 10.1364/opex.12.004490
30. Frazao, O. Curvature sensor using a highly birefringent photonic crystal fiber with two asymmetric hole regions in a Sagnac interferometer [Text] / O. Frazao, J. M. Baptista, J. L. Santos, P. Roy // *Applied Optics*. – 2008. – Vol. 47, Issue 13. – P. 2520–2523. doi: 10.1364/ao.47.002520
31. Andronova, I. A. Physical problems of fibergiroscope based on the Sagnac effect [Text] / I. A. Andronova, G. B. Malykin // *Physics-Uspexhi*. – 2002. – Vol. 45, Issue 8. – P. 793–817. doi: 10.1070/pu2002v045n08abeh001073
32. Shinde, Y. S. Gahir, Dynamic pressure sensing study using photonic crystal fiber: application to tsunami sensing [Text] / Y. S. Shinde, H. K. Gahir // *IEEE Photonics Technology Letters*. – 2008. – Vol. 20, Issue 4. – P. 279–281. doi: 10.1109/lpt.2007.913741
33. Ravi Kanth Kumar, V. V. Extruded soft glass photonic crystal fiber for ultrabroad supercontinuum generation [Text] / V. V. Ravi Kanth Kumar, A. George, W. Reeves, J. Knight, P. Russell, F. Omenetto, A. Taylor // *Opt. Express*. – 2002. – Vol. 10, Issue 25. – P. 1520. doi: 10.1364/oe.10.001520
34. Ebendorff-Heidepriem, H. Suspended nanowires: fabrication, design and characterization of fibers with nanoscale cores [Text] / H. Ebendorff-Heidepriem, S. C. Warren-Smith, T. M. Monro // *Opt. Express*. – 2009. – Vol. 17, Issue 4. – P. 2646. doi: 10.1364/oe.17.002646
35. Jiang, X. Single-mode hollow-core photonic crystal fiber made from sift glass [Text] / X. Jiang, T. G. Euser, F. Abdolvand, F. Babic, F. Tani, N. Y. Joly, J. C. Travers, P. St. J. Russell // *Optics express*. – 2011. – Vol. 19, Issue 16. – P. 15438–15444. doi: 10.1364/oe.19.015438
36. Jha, R. Ultrastable in reflection photonic crystal fiber modal interferometer for accurate refractive index sensing [Text] / R. Jha, J. Villatoro, G. Badenes // *Applied Physics Letters*. – 2008. – Vol. 93, Issue 19. – P. 191106:1–191106:3. doi: 10.1063/1.3025576
37. Jha, R. Refractometry based on a photonic crystal fiber interferometer [Text] / R. Jha, J. Villatoro, G. Badenes, V. Pruneri // *Optics Letters*. – 2009. – Vol. 34, Issue 5. – P. 617–619. doi: 10.1364/ol.34.000617
38. Cárdenas-Sevilla, G. A. Photonic crystal fiber sensor array based on modes overlapping [Text] / G. A. Cárdenas-Sevilla, V. Finazzi, J. Villatoro, V. Pruneri // *Optics Express*. – 2011. – Vol. 19, Issue 8. – P. 7596–7602. doi: 10.1364/oe.19.007596
39. Zhang, Y. Fringe visibility enhanced extrinsic Fabry-Perot interferometer using a graded index fiber collimator [Text] / Y. Zhang, Y. Li, T. Wei, X. Lan, Y. Huang, G. Chen, H. Xiao // *IEEE Photonics Journal*. – 2010. – Vol. 2, Issue 3. – P. 469–481. doi: 10.1109/jphot.2010.2049833
40. Tuchin, V. V. Sensornye svoystva fotonno-kristallicheskogo volnovoda s poloj serdcevinoy [Text] / V. V. Tuchin, Ju. S. Skibina, V. I. Beloglazov et. al. // *Pis'ma v ZhTF*. – 2008. – Vol. 34, Issue 15. – P. 63–69.
41. Russell, P. J. Photonic-Cristal Fibers [Text] / P. J. Russell // *Journal of Lightwave technology*. – 2006. – Vol. 24, Issue 12. – P. 4729–4749.
42. Fedotov, A. B. Volnovodnye svoystva i spektr sobstvennykh mod polyh fotonno-kristallicheskih volokon [Text] / A. B. Fedotov, S. O. Kononov, O. A. Koletovatova et. al. // *Kvantovaya jelektronika*. – 2003. – Vol. 33, Issue 3. – P. 271–274.
43. Chen, W. Ring-core photonic crystal fiber interferometer for strain measurement [Text] / W. Chen, S. Lou, L. Wang, S. Jian // *Optical Engineering*. – 2010. – Vol. 49, Issue 9. – P. 094402. doi: 10.1117/1.3488045
44. Mogilevtsev, D. Localized Function Method for Modelling Defect Modes in 2-d Photonic Crystals [Text] / D. Mogilevtsev, T. A. Birks, P. J. Russell // *Journal of lightwave technology*. – 1999. – Vol. 17, Issue 11. – P. 2078–2081. doi: 0.1109/50.802997